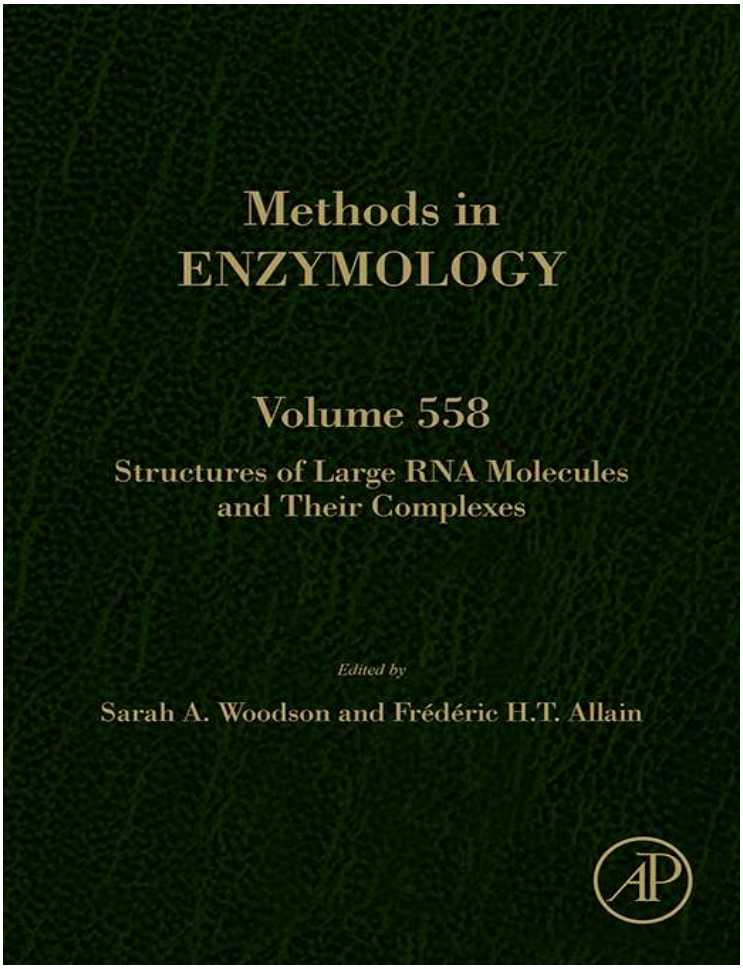

From Matthew L. Kahlscheuer, Julia Widom and Nils G. Walter, Single-Molecule Pull-Down FRET to Dissect the Mechanisms of Biomolecular Machines. In: Sarah A. Woodson and Frédéric H.T. Allain, editors, *Methods in Enzymology, Vol. 558*, Burlington: Academic Press, 2015, pp. 539-570.
ISBN: 978-0-12-801934-4

CHAPTER EIGHTEEN

Single-Molecule Pull-Down FRET to Dissect the Mechanisms of Biomolecular Machines

Matthew L. Kahlscheuer, Julia Widom, Nils G. Walter[1]
Single Molecule Analysis Group, Department of Chemistry, University of Michigan, Ann Arbor, Michigan, USA
[1]Corresponding author: e-mail address: nwalter@umich.edu

Contents

Abstract

Spliceosomes are multimegadalton RNA–protein complexes responsible for the faithful removal of noncoding segments (introns) from pre-messenger RNAs (pre-mRNAs), a process critical for the maturation of eukaryotic mRNAs for subsequent translation by the ribosome. Both the spliceosome and ribosome, as well as many other RNA and DNA processing machineries, contain central RNA components that endow biomolecular complexes with precise, sequence-specific nucleic acid recognition, and versatile structural dynamics. Single-molecule fluorescence (or Förster) resonance energy transfer (smFRET) microscopy is a powerful tool for the study of local and global conformational changes of both simple and complex biomolecular systems involving RNA. The integration of biochemical tools such as immunoprecipitation with advanced methods in smFRET microscopy and data analysis has opened up entirely new avenues toward studying the mechanisms of biomolecular machines isolated directly from complex

Methods in Enzymology, Volume 558
ISSN 0076-6879
http://dx.doi.org/10.1016/bs.mie.2015.01.009

biological specimens, such as cell extracts. Here, we detail the general steps for using prism-based total internal reflection fluorescence microscopy in exemplary single-molecule pull-down FRET studies of the yeast spliceosome and discuss the broad application potential of this technique.

1. INTRODUCTION

The spliceosome is the large protein–RNA complex responsible for the removal of introns from eukaryotic pre-messenger RNAs (pre-mRNAs) and the subsequent ligation of the remaining exons, generating continuous open reading frames that can be translated into protein (Wahl, Will, & Luhrmann, 2009). This process is a key step in gene expression, and defects in the splicing process are responsible for a significant fraction of known human genetic diseases (Wahl et al., 2009; Wang, Zhang, Li, Zhao, & Cui, 2012). Splicing consists of two chemical reactions, shown in Fig. 1A. In the first step of splicing, the 2′ hydroxyl group of the branchpoint adenosine attacks the phosphodiester backbone at the 5′ splice site, generating a free 5′ exon and a lariat intermediate containing the intron and the 3′ exon. In the second step, the liberated 3′ hydroxyl group of the 5′ splice site attacks a phosphate group at the 3′ splice site, expelling the intron lariat and ligating together the two exons. The spliceosome is rather unique among macromolecular machines in that it lacks a preformed active site and becomes catalytically active through assembly and rearrangement steps on the template of the pre-mRNA. In addition to the pre-mRNA substrate, splicing requires the RNA and protein components of five small nuclear ribonucleoprotein particles (snRNPs) and in humans, over 100 additional non-snRNP proteins (Fabrizio et al., 2009). The splicing cycle (Fig. 1B) proceeds through a specific sequence of binding, dissociation, and rearrangement events involving many of these protein and RNA components.

Any technique used to study a large, dynamic macromolecular complex such as the spliceosome must be sufficiently sensitive to detect low concentrations of sample, sufficiently specific to address a particular location of interest amid a large background of other protein and RNA components, and sufficiently information-rich to allow rigorous testing of mechanistic hypotheses. One technique that meets these requirements is single-molecule fluorescence (or Förster) resonance energy transfer (smFRET) (Förster, 1948; Roy, Hohng, & Ha, 2008; Stryer, 1978; Walter, 2003). In a FRET

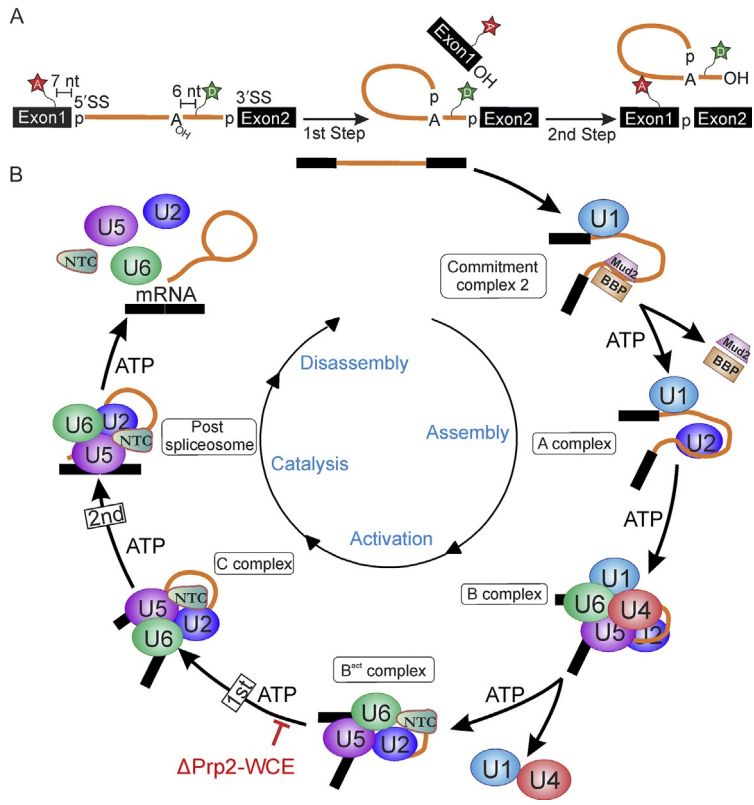

Figure 1 The canonical mechanism of pre-mRNA splicing catalyzed by the spliceosome. (A) The Ubc4 substrate contains donor (D, Cy3) and acceptor (A, Cy5) fluorophores near the BP and 5′SS, respectively, enabling observation of docking of the BP adenosine into the 5′SS during the first step of splicing. (B) Spliceosome assembly is thought to occur in a stepwise fashion with multiple ATP-dependent RNA–RNA and RNA–protein rearrangements between intermediary complexes, leading to the first and second chemical steps of splicing as indicated. In the Prp2-1,Cef1-TAP yeast strain, the B^{act} complex can be selectively formed through inactivation of the heat-sensitive ATPase Prp2 (red (gray in the print version) block).

experiment, a sample is labeled with a pair of fluorophores, chosen so that the emission spectrum of one (the "donor fluorophore") overlaps with the absorption spectrum of the other (the "acceptor fluorophore"). When the donor is excited, a dipole–dipole interaction between it and the acceptor permits the transfer of energy between the two, with the efficiency of this process depending on the distance and relative orientation between the two fluorophores, the fluorescence quantum yield of the donor, and the extent of spectral overlap between the donor's emission and the acceptor's absorption.

This distance dependence, which has a sensitivity range of ~10–100 Å, makes FRET a valuable technique for probing the conformations of biological macromolecules (Stryer, 1978; Walter, 2001, 2003). In smFRET, the molecule of interest is immobilized sparsely on a microscope slide so that the donor and acceptor fluorescence intensities, and thereby the FRET efficiency, can be measured for individual molecules (Roy et al., 2008). This is valuable because complex biological macromolecules often exist in multiple different conformations, and smFRET allows these conformations and their transitions to be observed, rather than reporting an ensemble average, which loses most of the information on transition kinetics, transient intermediates, and rare conformational states (Roy et al., 2008; Walter, Huang, Manzo, & Sobhy, 2008).

In recent years, smFRET has been applied to a number of protein–RNA complexes, including but not limited to the bacterial ribosome (Aitken, Petrov, & Puglisi, 2010; Chen, Tsai, O'Leary, Petrov, & Puglisi, 2012; Kim et al., 2014), the yeast spliceosome (Abelson, Blanco, et al., 2010; Crawford, Hoskins, Friedman, Gelles, & Moore, 2013; Krishnan et al., 2013), and human telomerase (Hwang et al., 2014; Parks & Stone, 2014). In most smFRET work, purified nucleic acid and protein components have been immobilized on slides through biotin–streptavidin linkages. Even the comparably small yeast spliceosome contains so many different components (five different snRNAs and ~40 different proteins, depending on the stage of splicing) (Fabrizio et al., 2009; Wahl et al., 2009) that it is not practical to purify every protein and RNA component in the spliceosome and reconstitute splicing "from scratch." Conversely, when working in cell extract, splicing can be stalled at many different stages of the splicing cycle using, for example, genetic manipulations that are readily available in yeast, leading to accumulation of certain intermediate complexes that can then be isolated and subjected to biochemical analysis. The gap between these two areas of inquiry (single-molecule observation of purified components and biochemical analysis of complexes isolated from cell extracts) was bridged by the technique of single-molecule pull-down (SiMPull), which was first demonstrated in 2011 (Jain, Liu, Xiang, & Ha, 2012; Jain et al., 2011). In this approach, a streptavidin-coated slide is incubated with a biotinylated antibody and extract is prepared from cells bearing a matching epitope, for example, a TAP or FLAG tag, on a protein of interest. This extract is incubated on the slide, allowing a particular complex to be "pulled down" from the extract onto the slide through the interaction between the antibody and the epitope. An extension of this approach termed SiMPull-FRET allows

complexes to be studied via smFRET that otherwise may be difficult to purify, immobilize, and/or reconstitute, and offers the potential for them to be studied in cell extract, offering relatively *in vivo*-like conditions (Krishnan et al., 2013).

In this chapter, we present the method of SiMPull-FRET, applied to the yeast spliceosome. First, we discuss the experimental methods required, including pre-mRNA preparation, the isolation of spliceosomal complexes for smFRET and for biochemical analysis, slide preparation and microscopy, and collection of smFRET data. Second, we discuss SiMPull-FRET data analysis, including histograms, hidden Markov modeling (HMM), and single-molecule cluster analysis. Finally, we present an application of SiMPull-FRET to the spliceosome in which the conformational fluctuations of the pre-mRNA before and during the first step of splicing were investigated (Krishnan et al., 2013).

2. EXPERIMENTAL METHODS

2.1 Labeling and purification of pre-mRNA substrates for smFRET

In order to study the complex dynamic behavior of pre-mRNA substrates throughout splicing using smFRET, molecules have to be site-specifically labeled with donor and acceptor fluorophores at positions along the RNA the distance of which is of particular interest to monitor. The selection of pre-mRNA substrate, location and choice of dyes, and method of immobilization must all be taken into account in order to produce a molecular ruler sufficient for monitoring important changes in RNA structure. A short, efficiently spliced pre-mRNA substrate, such as the yeast intron Ubc4 (Abelson, Blanco, et al., 2010), is ideal. Pre-mRNA splicing *in vitro* using yeast whole cell extract (WCE) is quite inefficient and may become even more inefficient upon introduction of large, hydrophobic fluorophores into the RNA. In addition, attachment of a moiety for immobilization, such as biotin, may restrict movement of the pre-mRNA substrate and further decrease splicing efficiency. Fortunately, splicing-specific microarray analysis, which utilizes hundreds of transcript-specific DNA probes capable of distinguishing pre-mRNA from mRNA, has recently made available the splicing efficiency of nearly all known yeast pre-mRNA substrates (Clark, Sugnet, & Ares, 2002; Pleiss, Whitworth, Bergkessel, & Guthrie, 2007). Thus, the list of suitable pre-mRNA substrates is reduced dramatically. In addition to splicing efficiency, the pre-mRNA length and structure must

also be taken into account. Total internal reflection fluorescence (TIRF) microscopy is limited to a depth of illumination of approximately 100–200 nm on the slide surface. More importantly, the synthesis and labeling of pre-mRNA substrates becomes increasingly difficult as the length of the RNA increases. As such, it is important to choose a pre-mRNA substrate short enough (<~400 nucleotides, nt) to be efficiently synthesized and labeled. Choosing a pre-mRNA substrate with significant secondary structure is also desired so that, depending upon the labeling sites, the assembly effects of the spliceosome (i.e., unfolding) can be observed through monitoring large changes in FRET efficiency. SHAPE-directed structure probing (McGinnis, Duncan, & Weeks, 2009) and structure prediction software provide a reasonable starting point in selecting the proper pre-mRNA substrate.

Once a pre-mRNA substrate has been chosen, optimal sites of labeling must next be chosen. Depending upon the desired experiment, FRET probes can be placed in such a way as to allow for the observation of particular assembly or catalytic steps in the splicing cycle. For example, fluorophores positioned near the 5′SS and BP allow for observation of docking of the BP adenosine near the 5′SS during the first step of splicing (Krishnan et al., 2013), while labeling near the 5′SS and 3′SS will allow for observation of docking of the 5′ exon near the intron–exon junction during the second step of splicing (Abelson, Blanco, et al., 2010). In either case, several sites should be tested to ensure the substrate splices with high efficiency upon incorporation of the donor and acceptor dyes. Many nucleotides and RNA sequences within a pre-mRNA (5′SS, BP, 3′SS, polypyrimidine tract, etc.) are evolutionarily conserved and participate in essential hydrogen bonding interactions with the spliceosome. Direct labeling of these sites should thus be avoided. In addition, particular structural motifs are often required for efficient splicing, further limiting the location of fluorescent probes. Taking all of these factors into account will ensure that addition of large, somewhat bulky fluorophores will have minimal effects on spliceosome assembly or catalysis.

There are several methods available for the site-specific, internal labeling of RNA with fluorophores for smFRET (Rinaldi, Suddala, & Walter, 2015; Solomatin & Herschlag, 2009; Walter, 2003; Walter & Burke, 2000). Chemical synthesis allows for incorporation of site-specific modifications and fluorophores directly during synthesis. Unfortunately, most pre-mRNA substrates are larger than 100 nt in length and thus exceed the typical length limitations of chemical synthesis of ~80 nt. Perhaps the most common method to overcome this limitation is to use splint-mediated RNA ligation

(Abelson, Blanco, et al., 2010; Abelson, Hadjivassiliou, & Guthrie, 2010; Crawford, Hoskins, Friedman, Gelles, & Moore, 2008; Krishnan et al., 2013; Moore & Query, 2000). In this approach, an RNA substrate is chemically synthesized in several segments, two of which contain aminoallyl uridine in the locations where the FRET probes are to be attached. Fluorophores are conjugated to the RNA by incubation with the *N*-hydroxysuccinimidyl ester fluorophore under slightly basic conditions. Unconjugated free dye is removed by ethanol precipitation of the RNA. Further purification of labeled from unlabeled RNA can be achieved by taking advantage of the hydrophobic nature of the attached fluorophore. Benzoylated naphthoylated DEAE-cellulose is a medium that has an affinity for hydrophobic material and thus will bind more tightly to fluorophore-containing RNA (Abelson, Blanco, et al., 2010; Krishnan et al., 2013). Fully conjugated RNA segments are then ligated together using DNA splints and RNA ligase 1, followed by polyacrylamide gel electrophoresis (PAGE) purification, yielding nearly 100% labeled RNA. Alternative methods of internal labeling include using the 10DM24 deoxyribozymes to site-specifically attach fluorophore-modified guanosine triphosphate analogs to specific adenosine residues on the *in vitro*-transcribed RNA backbone (Buttner, Javadi-Zarnaghi, & Hobartner, 2014). RNA length, structure, and location of adenosines can limit this method, and it is not yet clear whether the lariat-debranching enzyme found in yeast WCE may remove the label; however, it should provide a cheaper approach to labeling than chemical synthesis. If a longer pre-mRNA substrate is desired, labeling can be achieved through annealing of fluorescently labeled oligonucleotides to *in vitro*-transcribed pre-mRNA, as long as the resulting hybrid is sufficiently stable for the intended application (Fiegland, Garst, Batey, & Nesbitt, 2012).

A number of approaches also exist to modify and label the 5′ and 3′ ends of RNA (Ohrt et al., 2012; Qin & Pyle, 1999; Rinaldi et al., 2015). Incubation of RNA with sodium periodate results in the formation of 3′ aldehydes that can be conjugated with hydrazide derivatives of fluorophores or biotin (Newby Lambert et al., 2006). Alternatively, the free phosphate on the 5′ end of the RNA can be activated upon incubation with EDC (1-ethyl-3-[3-dimethylaminopropyl]carbodiimide hydrochloride). Incubation with imidazole and ethylenediamine produces the required primary amine for labeling with an NHS-ester fluorophore or biotin (Qin & Pyle, 1999; Rinaldi et al., 2015). Lastly, pre-mRNA transcripts can be 5′ end labeled through incorporation of 5′-GMPS (guanosine-5′-*O*-monophosphorothioate) during *in vitro* transcription followed by labeling

with maleimide-derivative fluorophores or biotin (Ohrt et al., 2012; Rueda, Hsieh, Day-Storms, Fierke, & Walter, 2005). While these methods of end-terminal labeling are efficient and relatively cost effective, labeling the 5′ or 3′ end of RNA does not offer the flexibility of internal labeling, potentially precluding the observation of important conformational dynamics required for assembly or catalysis.

A large number of fluorophores are available for smFRET studies, containing a variety of chemical properties (Roy et al., 2008). Perhaps, the most widely used FRET pair for the study of RNA dynamics is Cy3 and Cy5 (Abelson, Blanco, et al., 2010; Krishnan et al., 2013), although a number of improved derivatives are becoming increasingly available that exhibit increased photostability and higher quantum yield (Zheng et al., 2014). In addition, fluorophore lifetimes can be greatly increased by the use of an oxygen scavenging system (OSS), such as glucose, glucose oxidase, and catalase, or protocatechuic acid (PCA) and protocatechuate-3,4-dehydrogenase (PCD) (Aitken, Marshall, & Puglisi, 2008). In these systems, an enzyme and its substrate are added to the sample, chosen such that oxygen is consumed through the enzyme's reaction cycle. In addition, trolox is added as a triplet state quencher, which significantly reduces the occurrence of photoblinking. Care must be exercised when choosing the OSS for a particular smFRET experiment—for example, the addition of glucose to yeast WCE results in ATP depletion due to the action of endogenous hexokinase (Tatei, Kimura, & Ohshima, 1989), making PCA/PCD the preferred OSS for experiments performed in extract. Because fluorophore lifetimes are greatly reduced in the presence of the protein and RNA components within the splicing complex of interest as well as in the extract, choosing the proper FRET pair and OSS is crucial to an effective smFRET study. One interesting recent approach covalently attaches a triplet quencher directly to the fluorophore to affect "self-healing" through intramolecular triplet state quenching (Zheng et al., 2014); however, the added bulkiness of the so appended fluorophore has to be taken into consideration.

2.2 Isolation of splicing complexes through pull-down

Successful isolation and pull-down of a specific protein–protein or protein–RNA complex is central to the SiMPull-FRET methodology. SiMPull requires many of the same reagents that would be needed for coimmunoprecipitation experiments followed by Western blot analysis but is typically much cheaper, more sensitive, and less time consuming.

Selective pull-down is achieved through capture of a bait protein using a high-affinity antibody either specific for the bait protein itself or to a purification tag appended to the protein (TAP, Flag, etc.). The immobilized bait is then typically used to capture one or more, fluorescently labeled prey protein (as well as any interacting partners that might form a complex) in order to study stoichiometry of the bait–prey complex (Bharill, Fu, Palty, & Isacoff, 2014; Jain et al., 2011; Panter, Jain, Leonhardt, Ha, & Cresswell, 2012; Peterson et al., 2014; Shen et al., 2012) or conformational dynamics of a protein or protein complex (Zhou, Kunzelmann, Webb, & Ha, 2011; Zhou, Zhang, Bochman, Zakian, & Ha, 2014).

The bait-functionalized surface must specifically bind to the protein or complex of interest while rejecting all other biomolecules. In the case of SiMPull-FRET, the bait can be, for example, a TAP-tagged derivative of one of the components of the NineTeen Complex (NTC), Cef1, known to be present in the spliceosome during formation of the B^{act} complex (Lardelli, Thompson, Yates, & Stevens, 2010; Warkocki et al., 2009). The prey are the remaining protein, snRNA, and fluorescent substrate components known to be associated with the bait during B^{act} formation (Fig. 2A). As Cef1 does not interact with the spliceosome or the fluorescent pre-mRNA substrate prior to the B^{act} stage, any free Cef1 protein or Cef1-containing NTC that becomes captured by the antibody will not be visible upon Cy3 excitation.

The bait protein should be one that is stably associated within the larger complex (slow dissociation constant) to ensure that once immobilized, the larger complex will remain on the slide surface long enough for smFRET experimentation. Similarly, the antibody needs to feature high affinity together with slow epitope dissociation not to artificially shorten the observation of the immobilized complex, as well as exquisite specificity with little cross-reactivity with other WCE components. These requirements imply that not every Western blot validated antibody may work and that instead a more stringent selection criterion has to be applied such as suitability for immunofluorescence applications. In essence, pull-down of a complex onto a nonporous slide is a separation using only a single equilibrium binding stage (or "theoretical plate") that does not afford the benefits of, for example, an affinity purification column with its many theoretical plates that increase the separation efficiency between specifically and nonspecifically bound proteins. In addition, the bait should be known to join the spliceosome at a defined point in the assembly pathway and remains associated throughout all splicing steps of interest. Further enrichment for a specific splicing

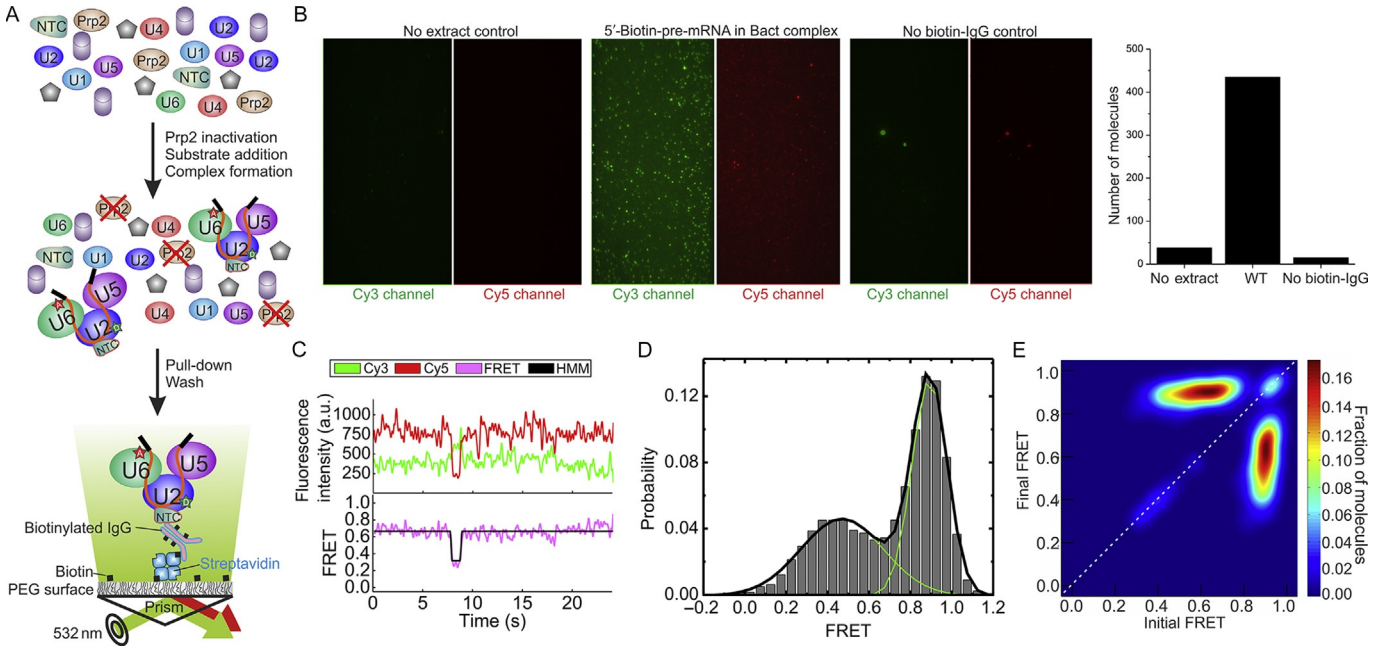

Figure 2 Schematic and analysis methodology of the SiMPull-FRET technique. (A) B^{act} complex formation is promoted through the heat inactivation of Prp2 prior to incubation of the whole cell extract with the fluorescent pre-mRNA substrate. Complexes are then pulled down for smFRET analysis on a biotin-PEG slide surface coated with streptavidin and biotinylated IgG antibody utilizing the TAP-tagged NTC component Cef1. (B) Representative fields of view showing the selective binding of the fluorescent substrate to the slide surface only when contained in the B^{act} complex and when slide surfaces have been saturated with IgG–biotin. Quantifications of the number of molecules binding under each slide condition are shown on the far right. (C) Representative Cy3 donor, Cy5 acceptor, FRET, and idealized hidden Markov model (HMM) traces from an smFRET experiment. (D) FRET probability distribution analysis used to determine the dominant FRET states of a population of single molecules. (E) Transition occupancy density plots (TODPs) are scaled by the fraction of all molecules that exhibit transitions from a particular initial FRET state (plotted along the *x*-axis) to a particular final FRET state (plotted along the *y*-axis). *Panel B was modified from Krishnan et al. (2013).*

intermediate is achieved through introduction of a biochemical or genetic stall known to arrest splicing at the assembly stage of interest. Fortunately, *Saccharomyces cerevisiae* is conducive to a host of genetic and biochemical modifications that allow for the introduction of point mutations and purification tags directly into the genome. Large yeast libraries are commercially available containing TAP and GFP tags on nearly every known protein. Of course, modern gene modification tools promise to make such tags much more readily available (Gaj, Gersbach, & Barbas, 2013; Tanenbaum, Gilbert, Qi, Weissman, & Vale, 2014). The IgG antibody–TAP interaction is one of the most specific protein–protein interactions, eliminating the need to raise antibodies to a protein of interest if one is not already available. In addition to the large availability and specificity, the IgG–TAP interaction provides a lengthy "spacer" between the splicing complex and the slide surface. It may be desired to isolate a particular complex and observe changes in FRET as spliceosomes progress through assembly and catalytic steps upon addition of the required proteins (Krishnan et al., 2013). Providing the spliceosome sufficient freedom to move about may improve the spliceosome's ability to function and progress along its assembly pathway on the slide surface.

Furthermore, years of experimentation have revealed a number of heat-sensitive and dominant-negative mutations in several essential splicing protein factors (Edwalds-Gilbert et al., 2000; Kim & Rossi, 1999; Plumpton, McGarvey, & Beggs, 1994; Schneider, Hotz, & Schwer, 2002; Vijayraghavan, Company, & Abelson, 1989). Heat-sensitive mutations allow for the inactivation of a protein component upon heating to the restricted temperature. Typically, the protein carrying this mutation is one required for progression beyond a specific assembly step in the splicing cycle. Yeast WCE from strains carrying the temperature-sensitive mutation can be made, allowing for the inactivation of the target protein prior to the *in vitro* splicing assay in much the same way that the strain itself is raised to a nonpermissive temperature. Once pre-mRNA substrate is introduced to this protein-inactivated extract, spliceosomes will accumulate at the assembly stage of interest. For example, B^{act} complex enrichment can be achieved through utilization of the Prp2-1,Cef1-TAP strain of yeast (Fig. 2A). Extract from this strain can be heated to the nonpermissive temperature, destroying the ATPase Prp2 required to progress beyond the B^{act} stage and preventing formation of complexes beyond B^{act}. Cef1 is known to only join the spliceosome upon B^{act} formation, thus preventing purification of pre-B^{act} complexes during TAP purification and thus leading to further enrichment

of the correct target on the slide (Fig. 1B; Lardelli et al., 2010). Alternatively, dominant-negative mutations are most typically introduced into a protein for recombinant overexpression and purification. Upon incubation of WCE with the recombinant mutant protein, splicing becomes stalled at the point where the wild-type protein is known to function. Both stalling techniques are known to be very efficient and allow for significant enrichment of a complex of interest. Finding the right combination of stalling and complex isolation will ensure a highly specific and efficient pull-down for smFRET.

2.2.1 Isolation of splicing complexes for biochemical control experiments

Regardless of the complex to be studied, biochemical verification of the specificity of complex isolation and function is required. Such biochemical validation may be as simple as isolating the RNA from the *in vitro*-assembled complex and looking for pre-mRNA, first-step, or second-step products via denaturing PAGE. For earlier assembly complexes (CC2, A, and B complexes), other verification approaches such as native gel analysis are required (Konarska, 1989; Legrain, Seraphin, & Rosbash, 1988). Alternatively, Northern and Western blot analyses can be used to identify which snRNAs and proteins, respectively, are assembled in the purified complex. For example, upon A complex formation, the presence of U1 and U2 snRNA would be expected, while U4/U6·U5 recruitment would not be expected until formation of the B complex or later.

A number of parameters must be optimized during this biochemical analysis phase to ensure efficient purification of a specific complex that is absent of all nonspecific binding partners. Because the pull-down itself will be performed on a slide surface, it is best to use conditions as similar as possible. One method is to use magnetic beads coated with streptavidin or neutravidin. Using a magnetic tube strip, the beads can easily be isolated from solution and washed of all unbound material. For example, in our work (Krishnan et al., 2013), streptavidin-coated beads were first incubated with biotinylated IgG, and subsequently, washed with a mild salt-containing buffer to remove excess antibody prior to incubation with yeast WCE containing the complex of interest. The immobilized complexes were then isolated by pulling the beads down using the magnetic strip and removing excess lysate with the supernatant. It is important to optimize the quantities of RNA, extract, and magnetic beads used to ensure efficient complex formation and isolation. In addition, complex formation may be performed prior to the addition of the beads to improve the efficiency of formation.

Removal of unbound and nonspecifically bound WCE components is perhaps the most crucial step to SiMPull-FRET. A suitable buffer should allow the complex to remain intact while removing protein and RNA loosely associated with the complex. Increasing salt concentrations and addition of mild detergents such as NP-40 will better remove nonspecifically bound components. However, it is important to verify the activity of the remaining complex upon washing. For situations in which a complex will be transitioning through assembly or catalytic steps upon addition of recombinant protein, wash steps must be stringent enough to prevent progression in the absence of recombinant proteins but mild enough to allow efficient transition (Krishnan et al., 2013).

Lastly, pre-mRNA and splicing products can be isolated from the magnetic beads using proteinase K digestion in order to remove all protein components of the spliceosome. Efficient degradation by proteinase K will result in release of the RNA into solution for retrieval by phenol–chloroform extraction and ethanol precipitation. Recovered material can then be dissolved and visualized via denaturing PAGE to identify the appropriate splicing intermediates or snRNA factors.

A general protocol for the purification of the B^{act} complex for biochemical validation purposes as performed in Krishnan et al. (2013) is as follows:

1. Inactivate Prp2-1,Cef1-TAP extract by heating at 37 °C for 45 min. Immediately place on ice
2. During extract inactivation, prepare streptavidin-coated magnetic beads (Dynabeads MyOne Streptavidin C1, Invitrogen)
   a. Equilibrate 200 μL of beads per 135 μL splicing reaction in T50 buffer (10 m*M* Tris–HCl, pH 8.0, 50 m*M* NaCl)
   b. Add an equal volume of 0.5 mg/mL biotin–IgG (ZyMAX rabbit anti-mouse IgG (H + L)—BT (ZyMAX Grade)) in T50 and incubate at room temperature (RT) for 30 min
   c. Pull-down the beads using a magnet and discard the supernatant
   d. (Optional) If using biotinylated pre-mRNA, incubate the beads with excess free biotin at 1.5 mg/mL in T50 buffer for 20 min at RT
   e. Pull-down beads, wash with T50, and equilibrate in splicing buffer
3. In a 135-μL reaction volume, incubate 40% (v/v) inactivated extract with 0.7–1.0 n*M* fluorescent pre-mRNA substrate and 2 m*M* ATP in splicing buffer (60 m*M* $K_i(PO_4)$, pH 7.0, 2 m*M* $MgCl_2$, 3% (w/v) poly(ethylene glycol) (PEG)) for 15 min at RT to allow accumulation of the B^{act} complex

4. Add complex formation reaction to prepared magnetic beads and continue to incubate at RT for 30 min
5. Pull-down beads and remove unbound supernatant
6. Thoroughly wash beads three times with wash buffer A (20 m*M* HEPES-KOH, pH 7.9, 120 m*M* KCl, 0.01% NP40, 1.5 m*M* $MgCl_2$, 5% (v/v) glycerol), and once with splicing buffer
7. For reconstitution with purified proteins, incubate beads with the proteins of interest (Prp2, Spp2, and Cwc25) at each 100 n*M* final concentration in splicing buffer in the presence of 2 m*M* ATP for 30 min at RT
8. Isolate pre-mRNA and splicing products by incubating each 200 μL splicing reaction with 30 m*M* EDTA, 0.5% SDS, and 20 μg Proteinase K (Life Technologies) at 42 °C for 20 min
9. Phenol–chloroform extract protein and ethanol precipitate RNA for analysis on a denaturing, 7 *M* urea, 15% polyacrylamide gel

2.2.2 Isolation of splicing complexes for smFRET

Isolation of the complex of interest for smFRET analysis is very similar to that for biochemical validation. Slide surfaces functionalized with a small amount of biotinylated PEG are first incubated with streptavidin, producing the functionalized surface that serves to take the place of the magnetic beads used for biochemical isolation. As with the biochemical purification, the slide surface is then coated with biotinylated IgG that will serve as the binding partner for the TAP-tagged splicing protein contained in the complex of interest. It is important to thoroughly wash away any unbound antibody to ensure all bait–prey complexes only bind to antibody coupled to the slide surface. A mild T50 buffer (10 m*M* Tris, pH 8.0, 50 m*M* NaCl) is usually sufficient for this step. Again, complex formation is typically performed in a test tube away from the slide to allow for unimpeded assembly on the fluorescent substrate. If formation reactions are flowed onto slides too early, the TAP-tagged protein will immediately start to become immobilized on the surface, restricting the space in which the complex can properly assemble. Conveniently, when using Cef1-TAP as the bait to isolate B^{act} any immobilized protein that has not been assembled into the proper splicing complex will lack fluorescence and thus be dark during the smFRET experiments. After each slide functionalization step, slide surfaces should be buffer exchanged into the buffer used for the subsequent immobilization in order to provide optimal conditions to support efficient binding of the complex of interest to the slide surface. Ideally, the surface density should be 300–400 molecules per field of view. A 100-μL reaction of 0.5–1 n*M* fluorescent Ubc4 incubated with 40% (v/v) Prp2-inactivated

WCE for 30 min was found to provide sufficient density upon introduction of the complex formation reaction to the slide surface (Krishnan et al., 2013). Depending on the efficiency of complex formation and the volume of the splicing reaction, it may also be necessary to test dilutions of the formation reaction to achieve proper single-molecule density on the slide surface. Complex formation reactions can also be allowed to incubate on the slide surface for a longer period of time until the proper surface density is achieved. Once the desired surface density is achieved, slide surfaces are washed with 300–400 μL of the previously optimized wash buffer to ensure removal of all nonspecifically bound complexes as well as loosely associated protein and RNA.

Several control experiments are required to verify the specificity of the pull-down. This is most easily and quickly performed on the slide surface because one simply has to detect enrichment in the number of fluorescent molecules bound to the slide surface in the presence of all binding partners. The required controls will primarily involve exclusion of the secondary antibody or binding partner responsible for identifying and pulling down the complex, a condition that should significantly reduce the number of binding events on the slide surface (Fig. 2B). Alternatively, inclusion of an alternative antibody lacking an affinity to the bait protein can serve as a negative control. In addition, when using biotinylated IgG as the bait binding partner, slides can be preincubated with Protein A, the target protein for the antibody. If slides are cleaned and functionalized properly, complex pull-down should be largely inhibited in the presence of excess Protein A.

A general protocol for the purification of the B^{act} complex for smFRET analysis as performed in Krishnan et al. (2013) is as follows:

1. Inactivate Prp2-1,Cef1-TAP extract by heating at 37 °C for 45 min. Immediately place on ice
2. In a 100-μL reaction volume, incubate 40% (v/v) inactivated extract with 0.7–1.0 n*M* fluorescent pre-mRNA substrate and 2 m*M* ATP in splicing buffer for 15 min at RT
3. Prepare functionalized slides (see Section 2.3.2)
   a. Hydrate PEGylated slides with 100 μL T50 buffer
   b. React slides with 0.2 mg/mL streptavidin in T50 buffer for 15 min. Wash slides with 100 μL T50 buffer
   c. Incubate slides with 100 μL of 0.5 mg/mL biotin–IgG in T50 buffer for 20 min
   d. (Optional) If using biotinylated pre-mRNA, incubate slide with free biotin at 1.5 mg/mL in T50 buffer for 15 min
   e. Wash slide with T50 and equilibrate in splicing buffer

4. Add complex formation reaction to prepared slide and continue to incubate until optimal density is achieved
5. Flow out splicing reaction with splicing buffer and wash extensively with 400 μL of wash buffer followed by equilibration in splicing buffer
6. If slide is to be imaged, include one further wash with splicing buffer containing the proper OSS
7. For reconstitution, incubate slide with the proteins of interest (Prp2, Spp2, and Cwc25) at a final concentration of 100 n*M* protein in splicing buffer, 2 m*M* ATP, and OSS

2.3 smFRET using prism-based TIRF microscopy

2.3.1 Summary of smFRET microscopy

Obtaining single-molecule sensitivity in a microscopy setup requires the separation of the desired signal from background. This is accomplished spectrally, by selecting optical filters that transmit only the red-shifted fluorescence emission of the fluorophore of interest, and spatially, by confining the excitation volume to the location where the fluorophore is immobilized. The latter is typically accomplished through TIRF microscopy (Axelrod, Burghardt, & Thompson, 1984), in which a laser beam is directed at the sample slide at an angle that generates total internal reflection at the glass–liquid interface. Under this condition, the laser generates an evanescent field within the liquid that penetrates only 50–150 nm from the interface (Axelrod et al., 1984; Walter et al., 2008), thus limiting the detected signal-to-fluorescence resulting from this region. This approach greatly enhances the signal detected from fluorophores immobilized on the slide surface relative to any that are in solution, significantly improving signal-to-background.

The basic optical setup for smFRET requires a laser to excite the donor fluorophore, an optional laser to excite the acceptor fluorophore, a microscope, optics to separate the donor and acceptor fluorescence signals, and a low-background camera such as an EMCCD (electron multiplying charge-coupled device). In many smFRET setups, total internal reflection is accomplished by directing the laser into a prism that sits on the microscope slide. Due to index matching oil placed between the prism and the slide, the laser is transmitted directly into the slide before undergoing total internal reflection at the slide–sample interface. Fluorescence is collected through the coverslip by a microscope objective, and a high-efficiency dichroic beamsplitter is used to separate donor and acceptor emission. Through the use of mirrors and a second dichroic, the donor and acceptor signals are redirected to be parallel but displaced from each other, and are imaged onto adjacent regions

of the active area of the EMCCD camera. Raw smFRET data consist of movies in which time-dependent images of the donor and acceptor regions of the camera are recorded while the donor fluorophore is being excited, and the intensity traces of individual points in each channel are then extracted (an example trace is shown in Fig. 2C). The details of further data analysis vary depending on the application and are detailed below.

2.3.2 Slide preparation and surface attachment

Because of the high sensitivity of single-molecule fluorescence microscopy, there are stringent requirements for the microscope slides and sample chambers used for imaging. Slides used for single-molecule fluorescence microscopy must be rigorously cleaned to remove any fluorescence contaminants that might otherwise contribute spurious signals. The surface of the slide must be passivated to prevent components of the sample, particularly proteins, from nonspecifically adhering to it. Finally, a means of immobilizing the sample on the slide surface must be incorporated into the slide preparation procedure (Roy et al., 2008). A variant of the latter procedure, briefly described here, was used for imaging B^{act} complex. The slide is boiled in water for 10 min, allowing tape, glue, and coverslips from previous experiments to be removed. It is then cleaned through sonication in Alconox detergent for 30 min, methanol for 10 min, and 1 *M* KOH for 20 min, and finally by boiling in "basic piranha solution," which consists of 14% (v/v) ammonium hydroxide and 4% (w/w) hydrogen peroxide in water. Aminosilanization of the slide surface is accomplished by immersing the slides in a 2% solution of (3-aminopropyl)triethoxysilane in acetone for 20 min with 1 min of sonication. The slides are then reacted for 2 h with a solution of 176 mg/mL NHS-ester functionalized PEG in 0.1 *M* sodium bicarbonate, including a 1:10 ratio of biotinylated to nonbiotinylated PEG. This step serves the dual purposes of passivating the slide surface against nonspecific binding and providing biotins that can later be used for sample immobilization. In a final step, the surface is reacted for 30 min with a solution of 20 mg/mL disulfosuccinimidyl tartrate (sulfo-DST) in 1 *M* sodium bicarbonate to passivate any unreacted amino groups. Sample chambers are constructed by attaching a coverslip to the slide using double-sided tape and sealing the ends with epoxy glue, and assembling tubing to allow sample to be injected into holes predrilled into the slide (Michelotti, de Silva, Johnson-Buck, Manzo, & Walter, 2010). As described above, the sample chamber is incubated with a solution of streptavidin immediately before use, allowing a biotinylated sample to be immobilized.

A general protocol for the preparation of PEG-modified slides for use in smFRET experiments follows. This procedure can be used to prepare new slides or regenerate used slides for repeated use. The volumes listed assume that one is preparing five slides at a time, and the assembly instructions assume that one is using a slide that already has two holes drilled into it, so that the sample chamber will run between the two holes. All steps are carried out at RT except where indicated.

1. Clean quartz slides
   - **a.** Boil in water for 10 min or until glue from previous use turns yellow. Use a razor blade to scrape off glue and coverslips
   - **b.** Make a thick paste with Alconox powder and a small amount of water. Use fingers to scrub each slide with paste for 30 s
   - **c.** Place slides in coplin jar with Alconox on slide surface. Fill with water, add 1 mL of concentrated cuvette cleaner, and sonicate for 30 min
   - **d.** Rinse with water and methanol, then sonicate for 10 min in methanol
   - **e.** Rinse with water, then sonicate for 20 min in 1 *M* KOH
   - **f.** Rinse with water, then boil for at least 20 min in basic Piranha solution (14% (w/v) NH_3 and 4% (w/v) H_2O_2 in water)
   - **g.** Rinse slides and coplin jar with water, then completely dry slides with N_2
2. Aminosilanate the slide surface
   - **a.** Rinse slides and coplin jar with acetone
   - **b.** Combine 70 mL acetone with 2 mL (3-aminopropyl)triethoxysilane (APTES) in coplin jar with slides
   - **c.** Incubate for 10 min, then sonicate for 1 min, and then incubate for 10 min
   - **d.** Rinse slides thoroughly with water, then dry slides completely with N_2
3. PEGylate the slide surface
   - **a.** Prepare empty pipette tip boxes to hold slides during reaction by cleaning and placing a small amount of water in the bottom to maintain a humid atmosphere
   - **b.** Prepare PEG reaction solution immediately before use by combining 8 mg biotin–PEG–succinimidyl valerate (MW 5000), 80 mg mPEG–succinimidyl valerate (MW 5000), and 500 μL PEGylation buffer (0.1 *M* $NaHCO_3$). Vortex to dissolve and centrifuge for 1 min at 10,000 rpm to pellet any undissolved material. Sterile filter using 0.2 μm syringe filter

   c. Place slides in prepared pipette tip boxes, pipette 70 μL of PEG solution onto the region of each slide that will form the sample chamber, and carefully place a coverslip over liquid, avoiding the formation of bubbles
   d. Incubate for at least 2 h in a dark place. Then rinse thoroughly with water and dry with N_2
4. React any remaining $-NH_2$ groups on the slide surface with disuccinimidyl tartarate (DST)
   a. Prepare DST reaction solution immediately before use by combining 10 mg DST with 500 μL DST buffer (1 *M* $NaHCO_3$). Vortex to dissolve and centrifuge for 1 min at 10,000 rpm to pellet any undissolved material. Sterile filter using 0.2 μm syringe filter
   b. Place slides in prepared pipette tip boxes, pipette 70 μL of DST solution onto each slide, and carefully place a coverslip over liquid, avoiding the formation of bubbles. Make sure to place the solution on the surface of the slide that the DST reaction solution was placed on
   c. Incubate for at least 30 min in a dark place. Then rinse thoroughly with water and dry with N_2
5. Assemble slide according to application. For example:
   a. Form a sample chamber between two strips of double-sided tape and place a coverslip over the tape. Make sure that the surface of the slide that was reacted with PEG and DST faces inward. Use epoxy to seal any edges that are not sealed by the double-sided tape
   b. Working on the opposite side of the slide, create inlet and outlet tubes by cutting pipette tips as needed to fit into the drilled holes and connecting the tips with rubber tubing. Use epoxy to seal the regions where the tips contact the slide and where the tubing contacts the tips
   c. Store slides in a dry, dark place

2.4 Experimental procedures for smFRET on the spliceosome

Once selective isolation and immobilization of the complex of interest have been achieved, SiMPull-FRET experiments are performed in a very similar manner to that of classical smFRET experiments. FRET is monitored through excitation of the donor fluorophore and detection of the subsequent fluorescence from the donor and acceptor fluorophores. As many complexes may contain only one of the two fluorophores (in its fluorescent

form), it will be important to include a direct excitation of the higher wavelength fluorophore near the end of the movie for a significant amount of time (at least 100 imaging frames on the camera). This allows low-FRET states to be distinguished from molecules that completely lack the acceptor fluorophore. In addition, donor excitation should be allowed to proceed until most of the field of view has bleached by the end of the observation to ensure identification of single complexes through single-step photobleaching. The detection of multiple photobleaching steps is usually attributable to the binding of two or more complexes very close to one another and FRET from these complexes should be ignored.

Due to the presence of extract or high concentrations of proteins, photobleaching will play a significant role in the longevity of the fluorophores. Observation times prior to photobleaching will last anywhere from seconds to several minutes depending upon the condition and concentration of protein, even in the presence of an efficient oxygen scavenging system. Laser power settings can be adjusted to extend the lifetime of the fluorophores. However, if the laser power is too low, the signal-to-noise will be very low making the confident identification of dynamics difficult. Several excitation laser powers should be tested in order to maximize fluorophore lifetime (>10 s) while still yielding a high enough signal-to-noise to detect FRET dynamics. Because of this short lifetime, it will also be important to record smFRET from at least five fields of view in order to gain good confidence in the data. For an equilibrium experiment, this can be done on the same slide, for a nonequilibrium (i.e., time-lapse) experiment, separate slides may have to be used.

The best smFRET experiments on the spliceosome will be those that allow for observation of progression through further assembly and catalytic steps upon addition of the required proteins and/or ATP (Krishnan et al., 2013). Having the ability to add a cofactor to release a specific block and thus "chase" splicing complexes through subsequent splicing steps opens up the door to experiments investigating proofreading, protein function, kinetics, etc. This ability can be confirmed during the biochemical validation experiments. However, dynamics and changes in dynamic behavior during smFRET experiments alone can often already be attributed to successful "chase" of protein–RNA complexes. The complex at equilibrium can be studied by incubation with the required proteins and ATP for 15 min prior to visualization. Alternatively, a progression in FRET states and the associated dynamics can be observed overtime as the protein acts on the isolated complexes by recording smFRET from several fields of view

immediately after protein addition. Once dynamic behaviors have been assigned to particular proteins, this activity can be confirmed through exclusion of ATP from the "chase" solution (in ATP-dependent processes) or addition of a mutant form of the added protein. Common yeast mutant proteins often are deficient in ATP binding, ATP hydrolysis, or protein/complex binding and as a result, become completely inactive.

3. DATA ANALYSIS

3.1 FRET histograms

One of the simplest ways to visualize a large number of smFRET traces in aggregate is to create a histogram (see Fig. 2D for an example). To create a histogram, the first step is to truncate each of the traces from a given experimental condition to its first 100 frames. This ensures that each trace contributes equally to the histogram, regardless of the total length of the trace (due to photobleaching, most molecules do not persist for the entire length of the movie, but they should persist for longer than 100 frames). All of the traces are combined into a single file in which the 100 frames contributed by each molecule are listed one after the other, with columns for time and FRET efficiency. This file is imported into a program such as OriginLab, in which the FRET efficiency values are grouped into discreet bins and the fraction of time spent in each FRET efficiency bin (collectively, between all of the traces considered) is determined. These data are displayed as a bar graph, indicating the relative frequency with which each bin of FRET states is observed. The histogram will typically include one or more peaks, whose centers and relative intensities can be estimated by fitting with the appropriate number of Gaussians. In Fig. 2D, for example, the FRET histogram indicates two populations, one with a broad range of FRET efficiencies centered near 0.5 and other with a narrow range of FRET efficiencies centered near 0.9.

3.2 HMM and transition occupancy density plot analysis

The histogram allows one to quickly determine the distribution of FRET states that are visited by the entire ensemble of molecules. The histogram says nothing, however, about transitions between the different populations observed. This information exists in the raw smFRET traces (as seen in Fig. 2C), but extracting it in a systematic way requires one to differentiate legitimate transitions from the noise that is inherent in single-molecule

measurements. One approach to this problem is the technique of HMM. When applied to smFRET, HMM requires the construction of a model that is defined by three probability matrices (Blanco & Walter, 2010). The "transition probability matrix" defines the probabilities of a given FRET state transitioning to another state in the next time step. The "emission probability matrix" defines the probability of a given FRET signal resulting from a given discreet FRET state. The "initiation probability matrix" defines the probability of a given trace starting in each of the possible FRET states. This model is "trained" on a dataset consisting of many individual molecules observed under a particular experimental condition, and the resulting optimization provides the model that best describes the data, as well as the most likely path between discreet FRET states in each single-molecule trace. This path is an "idealization" of the data, as shown in the lower panel of Fig. 2C, in which the fluctuating signal has been reduced to a series of discreet FRET states. In doing this, HMM clearly identifies transitions between different FRET states that may otherwise be hidden in noisy data.

HMM particularly shines when applied to complex systems like the spliceosome, in which many different FRET states are present, and it is difficult to identify transitions in a consistent and unbiased manner. Something as simple as the number of FRET states present can often be unclear in data such as these. In the work presented in the next section, the number of FRET states was determined by fitting the data using HMM models with different numbers of FRET states and using the Bayesian information criterion (BIC) to determine the appropriate number of states. BIC is based on both the likelihood score of the fit, which inevitably increases with an increasing number of states (and therefore fitting parameters), and a penalty term that increases with increasing number of parameters. Choosing the model with the number of FRET states that minimizes the BIC obtains a balance between model parsimony and likelihood score (Blanco & Walter, 2010).

One of the greatest benefits of HMM is that it clearly reveals transitions between different FRET states. The results of HMM can be presented in transition occupancy density plots (TODPs), which are two-dimensional plots indicating the fraction of molecules exhibiting at least one transition between a particular initial FRET efficiency (plotted along the x-axis) and a particular final FRET efficiency (plotted along the y-axis). An example is shown in Fig. 2E. In this plot, which was obtained from the same dataset as the histogram in Fig. 2D, a majority of molecules undergo transitions between FRET states centered at approximately 0.9 and 0.6. In addition,

a small population remains stably in the 0.9 FRET state and an even smaller population remains stably in the 0.6 FRET state. For each off-diagonal peak in the TODP, HMM yields a set of dwell times in the initial FRET state. These dwell times can be used to obtain the rate of each transition represented in the smFRET data. While TODPs offer a convenient visual representation of the dynamics of a population of molecules, rate constants allow quantitative comparison of the dynamics between different experimental conditions.

3.3 Postsynchronized histograms

Another analysis technique often employed for characterizing single-molecule behavior is postsynchronized histogram (PSH) analysis (Blanchard, Gonzalez, Kim, Chu, & Puglisi, 2004; Lee, Blanchard, Kim, Puglisi, & Chu, 2007; Senavirathne et al., 2012). PSHs are constructed by "postsynchronizing" smFRET time traces or HMM-fitted time trajectories to start at the first observation of a particular FRET state for every molecule in a certain condition. Trajectories are then binned within particular FRET bins and time windows to determine the number of trajectories located at a given FRET and time value. This approach is often used to remove the blurring effect resulting from asynchronous binding of a ligand to a target. By synchronizing all smFRET traces to the moment of the initial binding event, the subsequent changes in FRET can more easily be compared and the change in behavior of the entire population can more easily be inferred (Blanchard et al., 2004; Lee et al., 2007; Senavirathne et al., 2012). The initial starting FRET state can simply be a threshold of which FRET must be above or below, or a particular FRET efficiency. The constructed histograms can then be compiled to show how quickly a population progresses out of a particular FRET state. PSHs can also be applied to the data output of SiMPull-FRET (Krishnan et al., 2013). In this case, PSHs were constructed by synchronizing individual FRET events to the first occurrence of one of the macrostates. Such an approach allowed for a visually appealing method to determine whether a dataset was more likely to remain in the starting FRET state or transition to an alternative FRET state and, if so, how quickly this transition took place.

3.4 Clustering analysis

While histogram and TODP analyses provide the average dominant FRET conformations of a population of molecules as well as the most common

two-state transitions, these methods are not sufficient to provide an in-depth dissection of the complex dynamics often observed in smFRET studies. More complex systems often contain multiple interconverting FRET states with varying kinetics of transition between them. In addition, an ordered progression of states is often required for the proper function of many protein and RNA biomolecular machines. Unfortunately, techniques like TODP analysis assume that transitions are independent from one another, losing valuable information on molecules containing a characteristic series of transitions between multiple FRET states. Single-Molecule Cluster Analysis (SiMCAn) is a recently developed analysis tool capable of dissecting this complex behavior (Blanco et al., under review). SiMCAn utilizes hierarchical clustering from bioinformatics to group and sort complex smFRET traces based upon the FRET states present in a population as well as the kinetics between those FRET states. Interestingly, application of SiMCAn to a prior experimental dataset (Krishnan et al., 2013) produced similar conclusions to the previously only manually identified subpopulations of pre-mRNA molecules found to be within each splicing complex (Blanco et al., under review). SiMCAn thus promises to become a powerful analysis tool capable of unbiased extraction of the FRET states and multistep kinetics from single-molecule trajectories acquired using SiMPull-FRET.

4. THE SPLICEOSOME AS A BIASED BROWNIAN RATCHET MACHINE

SiMPull-FRET is a combination of classical smFRET and SiMPull. In an illustration of the type of mechanistic insight it can yield, it was used for a detailed analysis of the pre-mRNA conformational changes associated with the activation of the spliceosome during the first step of splicing (Krishnan et al., 2013). In this case, donor and acceptor fluorophores placed near the 5′SS and BP allowed for the observation of pre-mRNA conformational changes associated with the activity of specific proteins during progression of the B^{act} to the C complex. Utilizing a modified yeast strain, the B^{act} complex was selectively isolated from yeast WCE through inactivation of the ATPase Prp2 and affinity purification using a TAP-tagged Cef1 protein. Upon addition of the required recombinant proteins Prp2, Spp2, Cwc25, and ATP, protein and ATP-dependent changes in pre-mRNA conformation were observed, resulting from progression to the catalytically active B* intermediate and eventually the post-first-step C complex.

Histogram and TODP analysis of SiMPull-FRET data reveal that the isolated B^{act} complex remains locked in a static low-FRET state in which the 5′SS and BP are held stably apart from one another in order to prevent premature splicing activity (Fig. 3A–D, left column). Addition of Prp2, Spp2, and ATP (B* condition) resulted in the dynamic association of the BP with the 5′SS as indicated by rapid transitions from the low-FRET state of B^{act} into and out of a high-FRET state (Fig. 3A–D, center column). The ATPase activity of Prp2 is thought to weaken the binding of several BP-associated proteins (such as SF3a/b), proteins that presumably prevent the premature attack of the BP on the 5′SS. Accordingly, removal of such a complex would allow for the pre-mRNA to transiently and reversibly visit the higher FRET states indicative of a more proximal 5′SS and BP. Low levels of splicing are detected under these B* conditions, but only upon addition of Cwc25 do the 5′SS and BP become stably associated with one another (C condition), resulting in the significant enhancement in splicing efficiency observed in biochemical assays in the presence of Cwc25 (Fig. 3A–D, right column). Using smFRET between the pre-mRNA and protein, we found that Cwc25 binds near the BP, which then slows particularly the rate constant of the high- to mid-FRET transition, leading to longer dwell times in the precatalytic, stabilized high-FRET conformation required for first-step chemistry (Fig. 3E). PSH analysis showed that molecules under C complex conditions rapidly transition out of the M state and become stably locked in the H state (Fig. 3E). As a result, Cwc25 binding enhances the progression to the static high-FRET state associated with the postcatalytic C complex.

This behavior, observed using SiMPull-FRET, exemplifies how the spliceosome as a biomolecular machine couples chemical energy through ATP hydrolysis by the DExD/H-box helicase Prp2 into the release of a tightly bound road block ("pawl," in this case SF3a/b) stalling the B^{act} complex in a distal, low-FRET conformation. This release then allows for large-scale, intrinsic, random, and entirely thermally driven fluctuations of the pre-mRNA substrate in the B* complex (Fig. 4A). Such stochastic (Brownian) "ratcheting" is then rectified to produce directional ("biased") motion by introduction of a new, differently binding pawl (Cwc25) that brings the splice sites into close proximity and likely requires another helicase for its removal down the road. That is, chemical energy is primarily needed to set free the intrinsic conformational fluctuations of the substrate–spliceosome complex, followed by tight binding of a pawl to a newly accessible conformation, restricting motions again, and providing

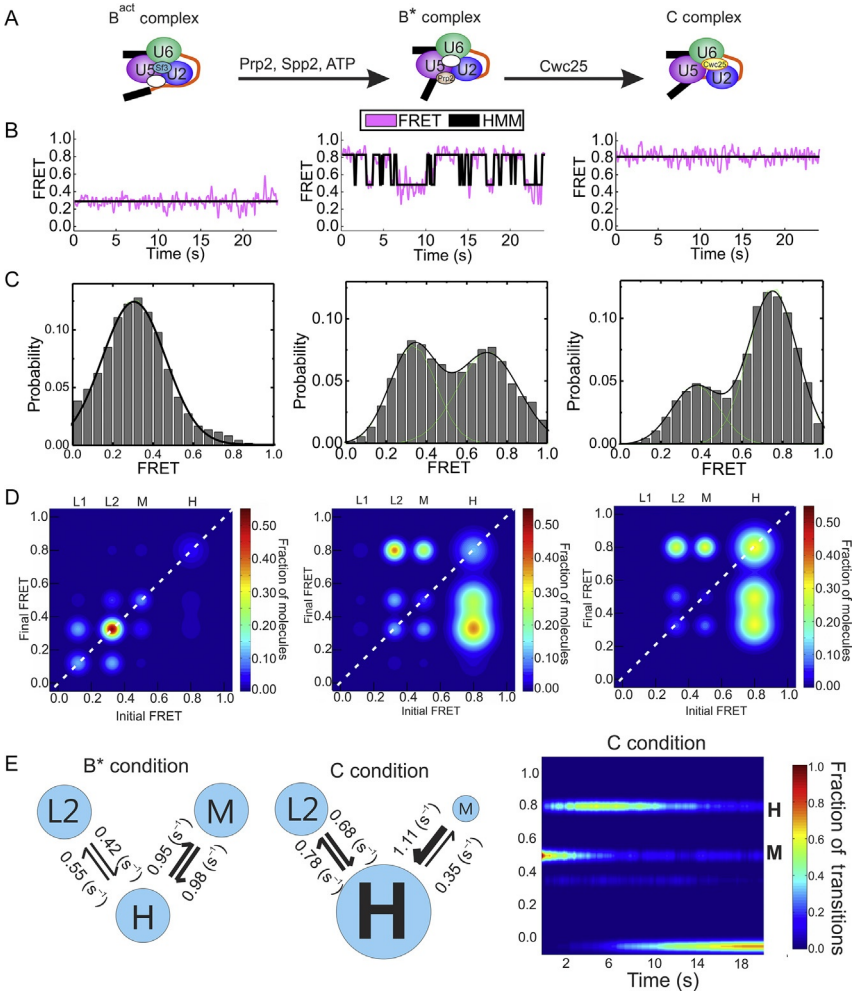

Figure 3 SiMPull-FRET analysis of the B^{act} complex. (A) The B^{act} complex is allowed to progress to the B* complex upon addition of Prp2, Spp2, and ATP, and then completes the first step of splicing into the C complex upon addition of Cwc25. (B–D) Representative FRET and idealized FRET (HMM) traces (B), FRET probability distributions (C), and TODPs (D) for the B^{act}, B*, and C complexes. (E) Kinetic analysis shows enrichment of the M-to-H transition under C complex conditions (middle) as compared to B* conditions (left). Postsynchronized histogram (PSH) showing rapid transition to, and stabilization of, the H state under C complex conditions. The accumulating zero FRET state represents the fraction of molecules that has photobleached overtime. *Modified from Krishnan et al. (2013).*

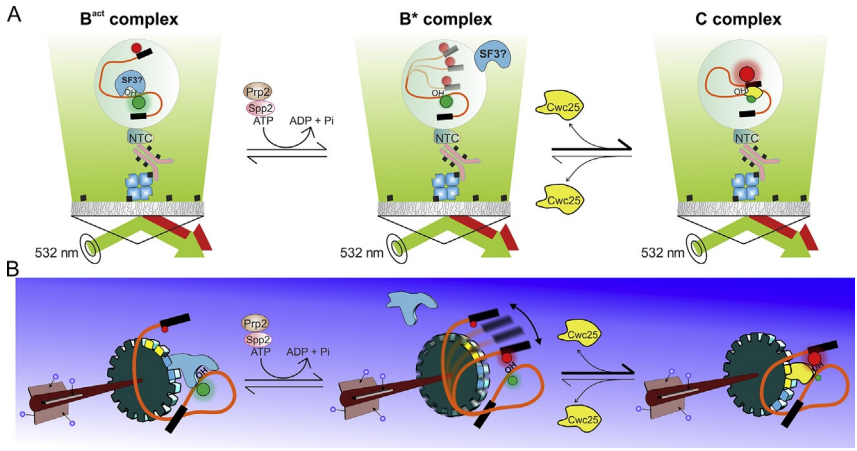

Figure 4 Biochemical (A) and mechanical (B) representations of the biased Brownian ratchet mechanism utilized by the spliceosome to promote first-step splicing. Binding of the SF3a/b complex (cyan) (gray in the print version) acts as a pawl to prevent docking of the BP and 5′SS in the B^{act} complex. Addition of Prp2, Spp2, and ATP results in the ATP-dependent release of SF3a/b from the spliceosome, allowing for dynamic docking and undocking of the 5′SS and BP and low levels of first-step splicing in the B* complex. Last, Cwc25 (yellow) (light gray in the print version) acts as a new pawl, stabilizing proximal 5′SS and BP in the C complex and allowing for more efficient first-step splicing.

directionality to the reaction pathway. Such a biased Brownian ratchet machine (Fig. 4B) was first envisioned by famed American physicist and Nobel laureate Richard Feynman. In this model, a gear is free to rotate in either direction due to random thermal fluctuations, but is held in place by a pawl (SF3a/b). An energy source releases this first pawl, allowing for the free, random rotation of the gear before once again becoming stalled at a new position through specific capture by a second pawl (Cwc25). Such a mechanism stands in stark contrast to the way most macroscopic machines function, such as a car engine, where burning of fossil fuel directly generates a force that propels the car forward by exploiting the inertia of its mechanical parts. A better macroscopic analogy for a biased Brownian ratchet machine may be a trapeze artist. The acrobat uses jump energy to propel off one platform, allowing intrinsic gravitational forces to freely carry them back and forth between the two platforms. Directional motion is achieved once the trapeze artist comes in contact with a second acrobat who catches them on the opposite platform. According to Feynman, a biased Brownian ratchet machine is the most likely process to affect directed motion at the nanoscale where neither inertia nor friction plays the dominant role they do in our macroscopic world (Feynman, 1963).

5. CONCLUSIONS AND OUTLOOK

Characterizing complex RNA and protein conformational changes is crucial to fully understand the function of large biomolecular machines. Here, we have provided details of how SiMPull-FRET integrates biochemical and biophysical approaches for the study of RNA-based machines like the spliceosome. Rather than purify every component of a complex system to reconstitute activity *in vitro*, SiMPull-FRET allows for the selective purification, immobilization, and characterization of macromolecular machines assembled from native components. As an example, application of SiMPull-FRET to selectively isolated, activated spliceosomes (B^{act} complex) allowed for the characterization of the pre-mRNA dynamics associated with the first step of splicing, revealing a biased Brownian ratcheting mechanism through which the spliceosome achieves efficient and accurate first-step splicing.

Conceivably, SiMPull-FRET can be used to study the pre-mRNA dynamics associated with most other splicing complexes using Ubc4 as the model substrate, although stages with helicase-driven conformational rearrangements, such as the Prp16- and Prp22-dependent rearrangements during the second catalytic step, will contain the most dynamic information and thus be most insightful. Most snRNA components are relatively short and are thus also suitable for fluorescent labeling in order to study snRNA–snRNA and snRNA–pre-mRNA rearrangements that are often critical for proper assembly and proofreading (Staley & Guthrie, 1998). In addition, such an approach could be used to more intimately study the mechanisms of alternative splicing in yeast and higher eukaryotic systems. In addition, as long as an efficient antibody and FRET fluorophore pair can be utilized for the system, SiMPull-FRET is suitable to study the mechanism of other molecular motor-driven processes from a variety of organisms, including—but not limited to—DNA replication, transcription, translation, DNA repair, chromatin dynamics, and RNA metabolism and export (Enguita & Leitao, 2014; von Hippel & Delagoutte, 2001).

As further RNA and protein labeling strategies become available that allow for the site-specific incorporation of ever improved donor and acceptor fluorophores and antibody–antigen interactions, we anticipate that SiMPull-FRET will become an increasingly valuable tool for identifying and quantifying the conformational dynamics associated with the folding and function of the individual proteins, RNAs, and large RNA–protein complexes that dominate the plethora of RNA-mediated processes in the eukaryotic cell (Pitchiaya, Heinicke, Custer, & Walter, 2014).

ACKNOWLEDGMENT

This work was supported by NIH Grant GM098023 to N.G.W.

REFERENCES

Abelson, J., Blanco, M., Ditzler, M. A., Fuller, F., Aravamudhan, P., Wood, M., et al. (2010). Conformational dynamics of single pre-mRNA molecules during in vitro splicing. *Nature Structural & Molecular Biology*, *17*(4), 504–512.

Abelson, J., Hadjivassiliou, H., & Guthrie, C. (2010). Preparation of fluorescent pre-mRNA substrates for an smFRET study of pre-mRNA splicing in yeast. *Methods in Enzymology*, *472*, 31–40.

Aitken, C. E., Marshall, R. A., & Puglisi, J. D. (2008). An oxygen scavenging system for improvement of dye stability in single-molecule fluorescence experiments. *Biophysical Journal*, *94*(5), 1826–1835.

Aitken, C. E., Petrov, A., & Puglisi, J. D. (2010). Single ribosome dynamics and the mechanism of translation. *Annual Review of Biophysics*, *39*, 491–513.

Axelrod, D., Burghardt, T. P., & Thompson, N. L. (1984). Total internal reflection fluorescence. *Annual Review of Biophysics and Bioengineering*, *13*, 247–268.

Bharill, S., Fu, Z., Palty, R., & Isacoff, E. Y. (2014). Stoichiometry and specific assembly of best ion channels. *Proceedings of the National Academy of Sciences of the United States of America*, *111*(17), 6491–6496.

Blanchard, S. C., Gonzalez, R. L., Kim, H. D., Chu, S., & Puglisi, J. D. (2004). tRNA selection and kinetic proofreading in translation. *Nature Structural & Molecular Biology*, *11*(10), 1008–1014.

Blanco, M. R., Martin, J., Kahlscheuer, M. L., Krishnan, R., Abelson, J., Laederach, A., et al. (2015). Single molecule cluster analysis identifies signature dynamic conformations along the splicing pathway. *Nature Methods*, under revision.

Blanco, M., & Walter, N. G. (2010). Analysis of complex single-molecule FRET time trajectories. *Methods in Enzymology*, *472*, 153–178.

Buttner, L., Javadi-Zarnaghi, F., & Hobartner, C. (2014). Site-specific labeling of RNA at internal ribose hydroxyl groups: Terbium-assisted deoxyribozymes at work. *Journal of the American Chemical Society*, *136*(22), 8131–8137.

Chen, J., Tsai, A., O'Leary, S. E., Petrov, A., & Puglisi, J. D. (2012). Unraveling the dynamics of ribosome translocation. *Current Opinion in Structural Biology*, *22*(6), 804–814.

Clark, T. A., Sugnet, C. W., & Ares, M., Jr. (2002). Genomewide analysis of mRNA processing in yeast using splicing-specific microarrays. *Science*, *296*(5569), 907–920.

Crawford, D. J., Hoskins, A. A., Friedman, L. J., Gelles, J., & Moore, M. J. (2008). Visualizing the splicing of single pre-mRNA molecules in whole cell extract. *RNA*, *14*(1), 170–179.

Crawford, D. J., Hoskins, A. A., Friedman, L. J., Gelles, J., & Moore, M. J. (2013). Single-molecule colocalization FRET evidence that spliceosome activation precedes stable approach of 5′ splice site and branch site. *Proceedings of the National Academy of Sciences of the United States of America*, *110*(17), 6783–6788.

Edwalds-Gilbert, G., Kim, D. H., Kim, S. H., Tseng, Y. H., Yu, Y., & Lin, R. J. (2000). Dominant negative mutants of the yeast splicing factor Prp2 map to a putative cleft region in the helicase domain of DExD/H-box proteins. *RNA*, *6*(8), 1106–1119.

Enguita, F. J., & Leitao, A. L. (2014). The art of unwinding: RNA helicases at the crossroads of cell biology and human disease. *Journal of Biochemical and Pharmacological Research*, *2*(3), 144–158.

Fabrizio, P., Dannenberg, J., Dube, P., Kastner, B., Stark, H., Urlaub, H., et al. (2009). The evolutionarily conserved core design of the catalytic activation step of the yeast spliceosome. *Molecular Cell*, *36*(4), 593–608.

Feynman, R. P. (1963). *The Feynman lectures on physics*. Massachusetts, USA: Addison-Wesley.
Fiegland, L. R., Garst, A. D., Batey, R. T., & Nesbitt, D. J. (2012). Single-molecule studies of the lysine riboswitch reveal effector-dependent conformational dynamics of the aptamer domain. *Biochemistry*, *51*(45), 9223–9233.
Förster, T. (1948). Zwischenmolekulare Energiewanderung Und Fluoreszenz. *Annalen der Physik*, *2*(1–2), 55–75.
Gaj, T., Gersbach, C. A., & Barbas, C. F., 3rd. (2013). ZFN, TALEN, and CRISPR/Cas-based methods for genome engineering. *Trends in Biotechnology*, *31*(7), 397–405.
Hwang, H., Kreig, A., Calvert, J., Lormand, J., Kwon, Y., Daley, J. M., et al. (2014). Telomeric overhang length determines structural dynamics and accessibility to telomerase and ALT-associated proteins. *Structure*, *22*(6), 842–853.
Jain, A., Liu, R., Ramani, B., Arauz, E., Ishitsuka, Y., Ragunathan, K., et al. (2011). Probing cellular protein complexes using single-molecule pull-down. *Nature*, *473*(7348), 484–488.
Jain, A., Liu, R., Xiang, Y. K., & Ha, T. (2012). Single-molecule pull-down for studying protein interactions. *Nature Protocols*, 7(3), 445–452.
Kim, H., Abeysirigunawarden, S. C., Chen, K., Mayerle, M., Ragunathan, K., Luthey-Schulten, Z., et al. (2014). Protein-guided RNA dynamics during early ribosome assembly. *Nature*, *506*(7488), 334–338.
Kim, D. H., & Rossi, J. J. (1999). The first ATPase domain of the yeast 246-kDa protein is required for in vivo unwinding of the U4/U6 duplex. *RNA*, *5*(7), 959–971.
Konarska, M. M. (1989). Analysis of splicing complexes and small nuclear ribonucleoprotein particles by native gel electrophoresis. *Methods in Enzymology*, *180*, 442–453.
Krishnan, R., Blanco, M. R., Kahlscheuer, M. L., Abelson, J., Guthrie, C., & Walter, N. G. (2013). Biased Brownian ratcheting leads to pre-mRNA remodeling and capture prior to first-step splicing. *Nature Structural & Molecular Biology*, *20*(12), 1450–1457.
Lardelli, R. M., Thompson, J. X., Yates, J. R., 3rd., & Stevens, S. W. (2010). Release of SF3 from the intron branchpoint activates the first step of pre-mRNA splicing. *RNA*, *16*(3), 516–528.
Lee, T. H., Blanchard, S. C., Kim, H. D., Puglisi, J. D., & Chu, S. (2007). The role of fluctuations in tRNA selection by the ribosome. *Proceedings of the National Academy of Sciences of the United States of America*, *104*(34), 13661–13665.
Legrain, P., Seraphin, B., & Rosbash, M. (1988). Early commitment of yeast pre-mRNA to the spliceosome pathway. *Molecular and Cellular Biology*, *8*(9), 3755–3760.
McGinnis, J. L., Duncan, C. D., & Weeks, K. M. (2009). High-throughput SHAPE and hydroxyl radical analysis of RNA structure and ribonucleoprotein assembly. *Methods in Enzymology*, *468*, 67–89.
Michelotti, N., de Silva, C., Johnson-Buck, A. E., Manzo, A. J., & Walter, N. G. (2010). A bird's eye view tracking slow nanometer-scale movements of single molecular nano-assemblies. *Methods in Enzymology*, *475*, 121–148.
Moore, M. J., & Query, C. C. (2000). Joining of RNAs by splinted ligation. *Methods in Enzymology*, *317*, 109–123.
Newby Lambert, M., Vocker, E., Blumberg, S., Redemann, S., Gajraj, A., Meiners, J. C., et al. (2006). Mg^{2+}-induced compaction of single RNA molecules monitored by tethered particle microscopy. *Biophysical Journal*, *90*(10), 3672–3685.
Ohrt, T., Prior, M., Dannenberg, J., Odenwalder, P., Dybkov, O., Rasche, N., et al. (2012). Prp2-mediated protein rearrangements at the catalytic core of the spliceosome as revealed by dcFCCS. *RNA*, *18*(6), 1244–1256.
Panter, M. S., Jain, A., Leonhardt, R. M., Ha, T., & Cresswell, P. (2012). Dynamics of major histocompatibility complex class I association with the human peptide-loading complex. *The Journal of Biological Chemistry*, *287*(37), 31172–31184.

Parks, J. W., & Stone, M. D. (2014). Coordinated DNA dynamics during the human telomerase catalytic cycle. *Nature Communications*, *5*, 4146.
Peterson, J. R., Labhsetwar, P., Ellermeier, J. R., Kohler, P. R., Jain, A., Ha, T., et al. (2014). Towards a computational model of a methane producing archaeum. *Archaea*, *2014*, 898453.
Pitchiaya, S., Heinicke, L. A., Custer, T. C., & Walter, N. G. (2014). Single molecule fluorescence approaches shed light on intracellular RNAs. *Chemical Reviews*, *114*(6), 3224–3265.
Pleiss, J. A., Whitworth, G. B., Bergkessel, M., & Guthrie, C. (2007). Transcript specificity in yeast pre-mRNA splicing revealed by mutations in core spliceosomal components. *PLoS Biology*, *5*(4), e90.
Plumpton, M., McGarvey, M., & Beggs, J. D. (1994). A dominant negative mutation in the conserved RNA helicase motif "SAT" causes splicing factor PRP2 to stall in spliceosomes. *The EMBO Journal*, *13*(4), 879–887.
Qin, P. Z., & Pyle, A. M. (1999). Site-specific labeling of RNA with fluorophores and other structural probes. *Methods*, *18*(1), 60–70.
Rinaldi, A. J., Suddala, K. C., & Walter, N. G. (2015). Native purification and labeling of RNA for single molecule fluorescence studies. *Methods in Molecular Biology*, *1240*, 63–95.
Roy, R., Hohng, S., & Ha, T. (2008). A practical guide to single-molecule FRET. *Nature Methods*, *5*(6), 507–516.
Rueda, D., Hsieh, J., Day-Storms, J. J., Fierke, C. A., & Walter, N. G. (2005). The 5′ leader of precursor tRNAAsp bound to the *Bacillus subtilis* RNase P holoenzyme has an extended conformation. *Biochemistry*, *44*(49), 16130–16139.
Schneider, S., Hotz, H. R., & Schwer, B. (2002). Characterization of dominant-negative mutants of the DEAH-box splicing factors Prp22 and Prp16. *The Journal of Biological Chemistry*, *277*(18), 15452–15458.
Senavirathne, G., Jaszczur, M., Auerbach, P. A., Upton, T. G., Chelico, L., Goodman, M. F., et al. (2012). Single-stranded DNA scanning and deamination by APOBEC3G cytidine deaminase at single molecule resolution. *The Journal of Biological Chemistry*, *287*(19), 15826–15835.
Shen, Z., Chakraborty, A., Jain, A., Giri, S., Ha, T., Prasanth, K. V., et al. (2012). Dynamic association of ORCA with prereplicative complex components regulates DNA replication initiation. *Molecular and Cellular Biology*, *32*(15), 3107–3120.
Solomatin, S., & Herschlag, D. (2009). Methods of site-specific labeling of RNA with fluorescent dyes. *Methods in Enzymology*, *469*, 47–68.
Staley, J. P., & Guthrie, C. (1998). Mechanical devices of the spliceosome: Motors, clocks, springs, and things. *Cell*, *92*(3), 315–326.
Stryer, L. (1978). Fluorescence energy transfer as a spectroscopic ruler. *Annual Review of Biochemistry*, *47*, 819–846.
Tanenbaum, M. E., Gilbert, L. A., Qi, L. S., Weissman, J. S., & Vale, R. D. (2014). *A protein-tagging system for signal amplification in gene expression and fluorescence imaging*. Cell.
Tatei, K., Kimura, K., & Ohshima, Y. (1989). New methods to investigate ATP requirement for pre-mRNA splicing: Inhibition by hexokinase/glucose or an ATP-binding site blocker. *Journal of Biochemistry*, *106*(3), 372–375.
Vijayraghavan, U., Company, M., & Abelson, J. (1989). Isolation and characterization of pre-mRNA splicing mutants of *Saccharomyces cerevisiae*. *Genes & Development*, *3*(8), 1206–1216.
von Hippel, P. H., & Delagoutte, E. (2001). A general model for nucleic acid helicases and their "coupling" within macromolecular machines. *Cell*, *104*(2), 177–190.
Wahl, M. C., Will, C. L., & Luhrmann, R. (2009). The spliceosome: Design principles of a dynamic RNP machine. *Cell*, *136*(4), 701–718.
Walter, N. G. (2001). Structural dynamics of catalytic RNA highlighted by fluorescence resonance energy transfer. *Methods*, *25*(1), 19–30.

Walter, N. G. (2003). Probing RNA structural dynamics and function by fluorescence resonance energy transfer (FRET). *Current Protocols in Nucleic Acid Chemistry,* Chapter 11, Unit 11.10.

Walter, N. G., & Burke, J. M. (2000). Fluorescence assays to study structure, dynamics, and function of RNA and RNA-ligand complexes. *Methods in Enzymology*, *317*, 409–440.

Walter, N. G., Huang, C. Y., Manzo, A. J., & Sobhy, M. A. (2008). Do-it-yourself guide: How to use the modern single-molecule toolkit. *Nature Methods*, *5*(6), 475–489.

Wang, J., Zhang, J., Li, K., Zhao, W., & Cui, Q. (2012). SpliceDisease database: Linking RNA splicing and disease. *Nucleic Acids Research*, *40*(Database issue), D1055–D1059.

Warkocki, Z., Odenwalder, P., Schmitzova, J., Platzmann, F., Stark, H., Urlaub, H., et al. (2009). Reconstitution of both steps of *Saccharomyces cerevisiae* splicing with purified spliceosomal components. *Nature Structural & Molecular Biology*, *16*(12), 1237–1243.

Zheng, Q., Juette, M. F., Jockusch, S., Wasserman, M. R., Zhou, Z., Altman, R. B., et al. (2014). Ultra-stable organic fluorophores for single-molecule research. *Chemical Society Reviews*, *43*(4), 1044–1056.

Zhou, R., Kunzelmann, S., Webb, M. R., & Ha, T. (2011). Detecting intramolecular conformational dynamics of single molecules in short distance range with subnanometer sensitivity. *Nano Letters*, *11*(12), 5482–5488.

Zhou, R., Zhang, J., Bochman, M. L., Zakian, V. A., & Ha, T. (2014). Periodic DNA patrolling underlies diverse functions of Pif1 on R-loops and G-rich DNA. *Elife*, *3*, e02190.